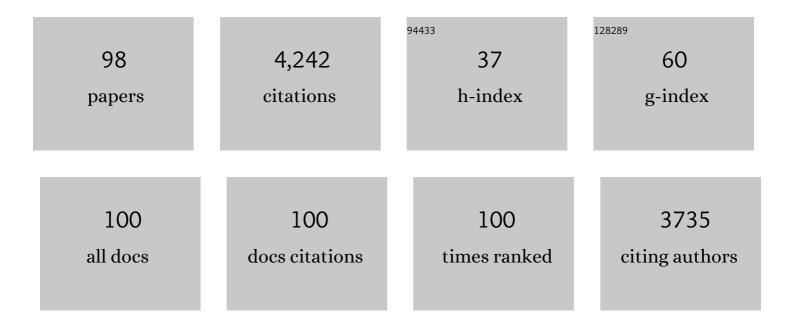
List of Publications by Year in descending order

Source: https://exaly.com/author-pdf/2882352/publications.pdf Version: 2024-02-01



Δρεμίο Μ.Διι

#	Article	IF	CITATIONS
1	Nipah (Musa Acuminata Balbisiana) banana peel as a lignocellulosic precursor for activated carbon: characterization study after carbonization process with phosphoric acid impregnated activated carbon. Biomass Conversion and Biorefinery, 2023, 13, 11085-11098.	4.6	13
2	Insight role of TiO <sub>2</sub> to improve the photocatalytic performance of WO <sub>3</sub> nanostructures for the efficient degradation of <i>ciprofloxacin</i> . Zeitschrift Fur Physikalische Chemie, 2022, 236, 169-180.	2.8	3
3	Investigating influential effect of methanolâ€phenolâ€steam mixture on hydrogen production through thermodynamic analysis with experimental evaluation. International Journal of Energy Research, 2022, 46, 964-979.	4.5	9
4	Effect of nonmetals (B, O, P, and S) doped with porous g-C3N4 for improved electron transfer towards photocatalytic CO2 reduction with water into CH4. Chemosphere, 2022, 286, 131765.	8.2	74
5	Recent developments in layered double hydroxide structures with their role in promoting photocatalytic hydrogen production: A comprehensive review. International Journal of Energy Research, 2022, 46, 2093-2140.	4.5	16
6	Influence of Ce substitution in LaMO3 (MÂ=ÂCo/Ni) perovskites for COx-free hydrogen production from ammonia decomposition. Arabian Journal of Chemistry, 2022, 15, 103547.	4.9	12
7	Single-step fabrication of highly stable amorphous TiO2 nanotubes arrays (am-TNTA) for stimulating gas-phase photoreduction of CO2 to methane. Chemosphere, 2022, 289, 133170.	8.2	18
8	Titanium Carbide MXene Nanostructures as Catalysts and Cocatalysts for Photocatalytic Fuel Production: A Review. ACS Applied Nano Materials, 2022, 5, 18-54.	5.0	41
9	Fabricating <scp> V <sub>2</sub> AlC </scp> / <scp> g  <sub>3</sub> N <sub>4</sub> </scp> nanocomposite with <scp>MAX</scp> as electron moderator for promoting photocatalytic <scp> CO <sub>2</sub> â€CH <sub>4</sub> </scp> refo. International Journal of Energy Research, 2022, 46, 7666-7685.	4.5	5
10	Sequential and/or Simultaneous Wet-Impregnation Impact on the Mesoporous Pt/Sn/Zn/γ-Al2O3 Catalysts for the Direct Ethane Dehydrogenation. Journal of Nanomaterials, 2022, 2022, 1-17.	2.7	2
11	Constructing S-Scheme Heterojunction of CoAlLa-LDH/g-C <sub>3</sub> N <sub>4</sub> through Monolayer Ti <sub>3</sub> C <sub>2</sub> -MXene to Promote Photocatalytic CO <sub>2</sub> Re-forming of Methane to Solar Fuels. ACS Applied Energy Materials, 2022, 5, 784-806.	5.1	38
12	Recent advances in constructing heterojunctions of binary semiconductor photocatalysts for visible light responsive <scp> CO <sub>2</sub> </scp> reduction to energy efficient fuels: A review. International Journal of Energy Research, 2022, 46, 5523-5584.	4.5	32
13	A review on sensitivity of operating parameters on biogas catalysts for selective oxidation of Hydrogen Sulfide to elemental sulfur. Chemosphere, 2022, 301, 134579.	8.2	7
14	The economic and environmental analysis of energy production from slaughterhouse waste in Saudi Arabia. Environment, Development and Sustainability, 2021, 23, 4252-4269.	5.0	11
15	Cellulose triacetate fiber-reinforced polystyrene composite. Journal of Thermoplastic Composite Materials, 2021, 34, 707-721.	4.2	9
16	Biodiesel production from novel non-edible caper (Capparis spinosa L.) seeds oil employing Cu–Ni doped ZrO2 catalyst. Renewable and Sustainable Energy Reviews, 2021, 138, 110558.	16.4	57
17	Well-designed 2D/2D Ti3C2TA/R MXene coupled g-C3N4 heterojunction with in-situ growth of anatase/rutile TiO2 nucleates to boost photocatalytic dry-reforming of methane (DRM) for syngas production under visible light. Applied Catalysis B: Environmental, 2021, 285, 119777.	20.2	132
18	Hydrothermal synthesis of an efficient and visible light responsive pure and strontium doped zinc oxide nano-hexagonal photocatalysts for photodegradation of Rhodamine B dye. Applied Nanoscience (Switzerland), 2021, 11, 1045-1056.	3.1	9

#	Article	IF	CITATIONS
19	Carbon Dioxide (CO <sub>2</sub> ) Capture in Alkanolamines Impregnated Activated Carbon Developed from Date Stones. Science of Advanced Materials, 2021, 13, 98-104.	0.7	6
20	Recent Developments in Natural Gas Flaring Reduction and Reformation to Energy-Efficient Fuels: A Review. Energy & Fuels, 2021, 35, 3675-3714.	5.1	63
21	Fabricating 2D/2D/2D heterojunction of graphene oxide mediated g-C3N4 and ZnV2O6 composite with kinetic modelling for photocatalytic CO2 reduction to fuels under UV and visible light. Journal of Materials Science, 2021, 56, 9985-10007.	3.7	18
22	Insighting role of activated carbon based nanostructures for complete photocatalytic degradation of hazardous pharmaceutical compound. Applied Nanoscience (Switzerland), 2021, 11, 1117-1126.	3.1	3
23	Role of Microalgae as a Source for Biofuel Production in the Future: A Short Review. Bulletin of Chemical Reaction Engineering and Catalysis, 2021, 16, 396-412.	1.1	9
24	Investigating the Influential Effect of Etchant Time in Constructing 2 <i>D</i> /2D HCN/MXene Heterojunction with Controlled Growth of TiO <sub>2</sub> NPs for Stimulating Photocatalytic H <sub>2</sub> Production. Energy & Fuels, 2021, 35, 6807-6822.	5.1	31
25	Synergistic Effect of Co/La in Oxygen Vacancy Rich Ternary CoAlLa Layered Double Hydroxide with Enhanced Reductive Sites for Selective Photoreduction of CO <sub>2</sub> to CH <sub>4</sub> . Energy & Fuels, 2021, 35, 8922-8943.	5.1	30
26	Polypropyleneâ€based nanocomposites for HVDC cable insulation. IET Nanodielectrics, 2021, 4, 84-97.	4.1	16
27	Mechanistic investigation of Mg2+-ion-induced ZnO nanorods for enhanced photocatalytic performance. Applied Nanoscience (Switzerland), 2021, 11, 1917-1927.	3.1	0
28	Structural, Thermal, Morphological and Magnetic Properties of Al3+-Doped Nanostructured Spinel Nickel Ferrites. Science of Advanced Materials, 2021, 13, 794-802.	0.7	1
29	Constructing La <sub><i>x</i></sub> Co <sub><i>y</i></sub> O <sub>3</sub> Perovskite Anchored 3D g-C <sub>3</sub> N <sub>4</sub> Hollow Tube Heterojunction with Proficient Interface Charge Separation for Stimulating Photocatalytic H <sub>2</sub> Production. Energy & amp; Fuels, 2021, 35, 9727-9746.	5.1	40
30	In-situ growth of TiO2 imbedded Ti3C2TA nanosheets to construct PCN/Ti3C2TA MXenes 2D/3D heterojunction for efficient solar driven photocatalytic CO2 reduction towards CO and CH4 production. Journal of Colloid and Interface Science, 2021, 591, 20-37.	9.4	71
31	Torrefaction and Thermochemical Properties of Agriculture Residues. Energies, 2021, 14, 4218.	3.1	7
32	Effect of Titanium oxide Nanofiller on the Electrical Properties of Polypropylene Nanocomposites for HVDC Insulation. , 2021, , .		1
33	Influence of van der waals heterostructures of 2D materials on catalytic performance of ZnO and its applications in energy: A review. International Journal of Hydrogen Energy, 2021, 46, 25413-25423.	7.1	14
34	First-principles calculations to investigate structural, electronic and optical properties of Na based fluoroperovskites NaXF3 (X= Sr, Zn). Solid State Communications, 2021, 334-335, 114396.	1.9	12
35	Current Trends and Approaches to Boost the Performance of Metal Organic Frameworks for Carbon Dioxide Methanation through Photo/Thermal Hydrogenation: A Review. Industrial & Engineering Chemistry Research, 2021, 60, 13149-13179.	3.7	34
36	Binary Ni <sub>2</sub> P/Ti <sub>3</sub> C <sub>2</sub> Multilayer Cocatalyst Anchored TiO <sub>2</sub> Nanocomposite with Etchant/Oxidation Grown TiO <sub>2</sub> NPs for Enhancing Photocatalytic H <sub>2</sub> Production. Energy & Fuels, 2021, 35, 14197-14211.	5.1	39

#	Article	IF	CITATIONS
37	Ammonia removal from raw water by using adsorptive membrane filtration process. Separation and Purification Technology, 2021, 270, 118757.	7.9	31
38	Photocatalytic CO2 reduction to CO and CH4 using g-C3N4/RGO on titania nanotube arrays (TNTAs). Journal of Materials Science, 2021, 56, 18989-19014.	3.7	14
39	Advances in structural modification of perovskite semiconductors for visible light assisted photocatalytic CO2 reduction to renewable solar fuels: A review. Journal of Environmental Chemical Engineering, 2021, 9, 106264.	6.7	56
40	Structural, electronics and optical properties of sodium based fluoroperovskites NaXF3 (X = Ca, Mg, Sr) Tj I Physics, 2021, 412, 127574.	ETQq0 0 ( 2.1	0 rgBT /Overloo 31
41	Novel, facile and first time synthesis of zinc oxide nanoparticles using leaves extract of Citrus reticulata for photocatalytic and antibacterial activity. Optik, 2021, 243, 167495.	2.9	14
42	Capacitive properties of novel Sb-doped Co3O4 electrode material synthesized by hydrothermal method. Ceramics International, 2021, 47, 32210-32217.	4.8	6
43	Facile fabrication of well-designed 2D/2D porous g-C3N4–GO nanocomposite for photocatalytic methane reforming (DRM) with CO2 towards enhanced syngas production under visible light. Fuel, 2021, 305, 121558.	6.4	44
44	Functionalized role of highly porous activated carbon in bismuth vanadate nanomaterials for boosted photocatalytic hydrogen evolution and synchronous activity in water. International Journal of Hydrogen Energy, 2021, 46, 39778-39785.	7.1	8
45	Synthesis of BiVO4/NiFe2O4 composite for photocatalytic degradation of methylene blue. Applied Nanoscience (Switzerland), 2021, 11, 2793.	3.1	7
46	Construction of an S-Scheme Heterojunction with Oxygen-Vacancy-Rich Trimetallic CoAlLa-LDH Anchored on Titania-Sandwiched Ti <sub>3</sub> C <sub>2</sub> Multilayers for Boosting Photocatalytic CO <sub>2</sub> Reduction under Visible Light. Industrial & Engineering Chemistry Research, 2021, 60, 16201-16223.	3.7	33
47	Role of Ti <sub>3</sub> C <sub>2</sub> MXene as Prominent Schottky Barriers in Driving Hydrogen Production through Photoinduced Water Splitting: A Comprehensive Review. ACS Applied Energy Materials, 2021, 4, 11982-12006.	5.1	57
48	Doped Nanostructured Manganese Ferrites: Synthesis, Characterization, and Magnetic Properties. Journal of Nanomaterials, 2021, 2021, 1-12.	2.7	5
49	Template free synthesis of graphitic carbon nitride nanotubes mediated by lanthanum (La/g-CNT) for selective photocatalytic CO2 reduction via dry reforming of methane (DRM) to fuels. Applied Surface Science, 2020, 504, 144177.	6.1	83
50	MgFe and Mg–Co–Fe mixed oxides derived from hydrotalcites: Highly efficient catalysts for COx free hydrogen production from NH3. International Journal of Hydrogen Energy, 2020, 45, 873-890.	7.1	28
51	Tailoring metal/support interaction in 0D TiO2 NPs/MPs embedded 2D MAX composite with boosted interfacial charge carrier separation for stimulating photocatalytic H2 production. Journal of Environmental Chemical Engineering, 2020, 8, 104529.	6.7	10
52	Constructing a Stable 2D Layered Ti <sub>3</sub> C <sub>2</sub> MXene Cocatalyst-Assisted TiO <sub>2</sub> /g-C <sub>3</sub> N <sub>4</sub> /Ti <sub>3</sub> C <sub>2</sub> Heterojunction for Tailoring Photocatalytic Bireforming of Methane under Visible Light. Energy & Fuels, 2020, 34, 9810-9828.	5.1	84
53	Well-Designed 3D/2D/2D WO <sub>3</sub> /Bt/g-C <sub>3</sub> N <sub>4</sub> Z-Scheme Heterojunction for Tailoring Photocatalytic CO <sub>2</sub> Methanation with 2D-Layered Bentonite-Clay as the Electron Moderator under Visible Light. Energy & Fuels, 2020, 34, 14400-14418.	5.1	40
54	Photoinduced Dry and Bireforming of Methane to Fuels over Laâ€Modified TiO <sub>2</sub> in Fixedâ€Bed and Monolith Reactors. Energy Technology, 2020, 8, 2000106.	3.8	11

#	Article	IF	CITATIONS
55	Recent development in band engineering of binary semiconductor materials for solar driven photocatalytic hydrogen production. International Journal of Hydrogen Energy, 2020, 45, 15985-16038.	7.1	187
56	Highly efficient hydrotalcite supported palladium catalyst for hydrodechlorination of 1, 2, 4-tri chlorobenzene: Influence of Pd loading. Journal of Chemical Sciences, 2020, 132, 1.	1.5	2
57	Construction of a Stable Two-Dimensional MAX Supported Protonated Graphitic Carbon Nitride (pg-C <sub>3</sub> N <sub>4</sub> )/Ti <sub>3</sub> AlC <sub>2</sub> /TiO <sub>2</sub> Z-Scheme Multiheterojunction System for Efficient Photocatalytic CO <sub>2</sub> Reduction through Dry Reforming of Methanol. Energy & amp: Fuels, 2020, 34, 3540-3556.	5.1	77
58	Enhanced photocatalytic CO2 reduction to fuels through bireforming of methane over structured 3D MAX Ti3AlC2/TiO2 heterojunction in a monolith photoreactor. Journal of CO2 Utilization, 2020, 38, 99-112.	6.8	47
59	Bimetallic Ruâ€Fe Nanoparticles Supported on Carbon Nanotubes for Ammonia Decomposition and Synthesis. Chemical Engineering and Technology, 2020, 43, 719-730.	1.5	26
60	Correlation Between Tunable Oxygen Defects in TiO <sub>2</sub> Nanoflower and Its Photocatalytic Performance for the Degradation of Organic Waste. Nano, 2020, 15, 2050018.	1.0	3
61	In-situ synthesis of TiO2/La2O2CO3/rGO composite under acidic/basic treatment with La3+/Ti3+ as mediators for boosting photocatalytic H2 evolution. International Journal of Hydrogen Energy, 2019, 44, 23669-23688.	7.1	20
62	Facile synthesis of GO and g-C3N4 nanosheets encapsulated magnetite ternary nanocomposite for superior photocatalytic degradation of phenol. Environmental Pollution, 2019, 253, 1066-1078.	7.5	50
63	Ag-La loaded protonated carbon nitrides nanotubes (pCNNT) with improved charge separation in a monolithic honeycomb photoreactor for enhanced bireforming of methane (BRM) to fuels. Applied Catalysis B: Environmental, 2019, 248, 167-183.	20.2	79
64	Characterization of an amorphous indium tin oxide (ITO) film on a polylactic acid (PLA) substrate. Bulletin of Materials Science, 2019, 42, 1.	1.7	6
65	Engineering approach to enhance photocatalytic water splitting for dynamic H2 production using La2O3/TiO2 nanocatalyst in a monolith photoreactor. Applied Surface Science, 2019, 484, 1089-1101.	6.1	56
66	Cu-NPs embedded 1D/2D CNTs/pCN heterojunction composite towards enhanced and continuous photocatalytic CO2 reduction to fuels. Applied Surface Science, 2019, 485, 450-461.	6.1	77
67	Methanol Synthesis Using CO <sub>2</sub> and H <sub>2</sub> on Nano Silver-Ceria Zirconia Catalysts: Influence of Preparation Method. Journal of Nanoscience and Nanotechnology, 2019, 19, 3197-3204.	0.9	6
68	Sub-3 nm Rh nanoclusters confined within a metal–organic framework for enhanced hydrogen generation. Chemical Communications, 2019, 55, 4699-4702.	4.1	32
69	Montmorillonite dispersed single wall carbon nanotubes (SWCNTs)/TiO2 heterojunction composite for enhanced dynamic photocatalytic H2 production under visible light. Applied Clay Science, 2019, 174, 110-119.	5.2	40
70	Indirect Z-Scheme Assembly of 2D ZnV <sub>2</sub> O <sub>6</sub> /RGO/g-C <sub>3</sub> N <sub>4</sub> Nanosheets with RGO/pCN as Solid-State Electron Mediators toward Visible-Light-Enhanced CO <sub>2</sub> Reduction. Industrial & Engineering Chemistry Research, 2019, 58, 8612-8624.	3.7	84
71	Comprehensive dynamic modeling, simulation, and validation for an industrial boiler incident investigation. Process Safety Progress, 2019, 38, e12040.	1.0	4
72	Carbon Nanotubes Incorporated Z-Scheme Assembly of AgBr/TiO2 for Photocatalytic Hydrogen Production under Visible Light Irradiations. Nanomaterials, 2019, 9, 1767.	4.1	14

#	Article	IF	CITATIONS
73	Recent advancements in engineering approach towards design of photo-reactors for selective photocatalytic CO2 reduction to renewable fuels. Journal of CO2 Utilization, 2019, 29, 205-239.	6.8	189
74	Enhanced photocatalytic carbon dioxide reforming of methane to fuels over nickel and montmorillonite supported TiO2 nanocomposite under UV-light using monolith photoreactor. Journal of Cleaner Production, 2019, 213, 451-461.	9.3	93
75	Hierarchical 3D VO2/ZnV2O4 microspheres as an excellent visible light photocatalyst for CO2 reduction to solar fuels. Applied Surface Science, 2019, 467-468, 1170-1180.	6.1	69
76	La-modified TiO2/carbon nanotubes assembly nanocomposite for efficient photocatalytic hydrogen evolution from glycerol-water mixture. International Journal of Hydrogen Energy, 2019, 44, 3711-3725.	7.1	76
77	Well-designed ZnV2O6/g-C3N4 2D/2D nanosheets heterojunction with faster charges separation via pCN as mediator towards enhanced photocatalytic reduction of CO2 to fuels. Applied Catalysis B: Environmental, 2019, 242, 312-326.	20.2	162
78	Tailoring performance of La-modified TiO 2 nanocatalyst for continuous photocatalytic CO 2 reforming of CH 4 to fuels in the presence of H 2 O. Energy Conversion and Management, 2018, 159, 284-298.	9.2	90
79	Ethyl benzene oxidative dehydrogenation to styrene on Al-B and Al-B-Sb catalysts. Applied Catalysis A: General, 2018, 552, 49-57.	4.3	6
80	Implication of iron nitride species to enhance the catalytic activity and stability of carbon nanotubes supported Fe catalysts for carbon-free hydrogen production <i>via</i> low-temperature ammonia decomposition. Catalysis Science and Technology, 2018, 8, 907-915.	4.1	46
81	Impact of cobalt as dopant on surface morphologies of undoped <scp>ZnO</scp> nanostructured thin films. Asia-Pacific Journal of Chemical Engineering, 2018, 13, e2183.	1.5	1
82	Cold plasma dielectric barrier discharge reactor for dry reforming of methane over Ni/ɤl2O3-MgO nanocomposite. Fuel Processing Technology, 2018, 178, 166-179.	7.2	77
83	Size structure–catalytic performance correlation of supported Ni/MCF-17 catalysts for CO <sub>x</sub> -free hydrogen production. Chemical Communications, 2018, 54, 6364-6367.	4.1	36
84	Synthesis and Characterization of Pentaerythritol Phthalic Anhydride Resin from Soybean Oil. Asian Journal of Chemistry, 2018, 30, 572-574.	0.3	2
85	Photo-induced CO2 reduction by CH4/H2O to fuels over Cu-modified g-C3N4 nanorods under simulated solar energy. Applied Surface Science, 2017, 419, 875-885.	6.1	140
86	Synergistic effect in plasmonic Au/Ag alloy NPs co-coated TiO2 NWs toward visible-light enhanced CO2 photoreduction to fuels. Applied Catalysis B: Environmental, 2017, 204, 548-560.	20.2	231
87	Effect of preparation methods on the catalyst performance of Co/Mg La mixed oxide catalyst for COx-free hydrogen production by ammonia decomposition. International Journal of Hydrogen Energy, 2017, 42, 24213-24221.	7.1	30
88	Selective photocatalytic reduction of CO2 by H2O/H2 to CH4 and CH3OH over Cu-promoted In2O3/TiO2 nanocatalyst. Applied Surface Science, 2016, 389, 46-55.	6.1	129
89	Daily variation of radon gas and its short-lived progeny concentration near ground level and estimation of aerosol residence time. Chinese Physics B, 2016, 25, 050701.	1.4	4
90	Photocatalytic CO2 conversion over Au/TiO2 nanostructures for dynamic production of clean fuels in a monolith photoreactor. Clean Technologies and Environmental Policy, 2016, 18, 2147-2160.	4.1	21

#	Article	IF	CITATIONS
91	Kinetics of hydrogen adsorption on MgH2/CNT composite. Materials Research Bulletin, 2016, 77, 23-28.	5.2	41
92	Effect of Au Precursor and Support on the Catalytic Activity of the Nano-Au-Catalysts for Propane Complete Oxidation. Journal of Nanomaterials, 2015, 2015, 1-10.	2.7	3
93	Gold–indium modified TiO2 nanocatalysts for photocatalytic CO2 reduction with H2 as reductant in a monolith photoreactor. Applied Surface Science, 2015, 338, 1-14.	6.1	86
94	Strong synergism between gold and manganese in an Au–Mn/triple-oxide-support (TOS) oxidation catalyst. Applied Catalysis A: General, 2015, 489, 24-31.	4.3	13
95	Conventional versus lattice photocatalysed reactions: Implications of the lattice oxygen participation in the liquid phase photocatalytic oxidation with nanostructured ZnO thin films on reaction products and mechanism at both 254nm and 340nm. Applied Catalysis B: Environmental, 2011, 106, 323-336.	20.2	34
96	Photocatalysis with nanostructured zinc oxide thin films: The relationship between morphology and photocatalytic activity under oxygen limited and oxygen rich conditions and evidence for a Mars Van Krevelen mechanism. Applied Catalysis B: Environmental, 2010, 97, 168-181.	20.2	116
97	H2-rich syngas production from air gasification of date palm waste: an experimental and modeling investigation. Biomass Conversion and Biorefinery, 0, , 1.	4.6	14
98	MOF-Based Catalysts for Production of Value-Added Fine Chemicals from Carbon Dioxide. ACS Symposium Series, 0, , 155-171.	0.5	4